

Performance of Landsat 8 and Sentinel 2A in vegetation cover mapping of Ise Forest Reserve, Southwest Nigeria

✉ Olaniyi, O.E.¹, Adegbola, O.O.¹ and Adefurin, O.M.²

¹Department of Ecotourism and Wildlife Management, Federal University of Technology, Akure, Nigeria. ²Tennessee State University, 330 10th Avenue North, Nashville, TN 37203, United States of America. ✉ Corresponding author: oeolaniyi@futa.edu.ng +2348069266810

Accepted on June 29, 2020.

Abstract

In recent years, the high cost and non-affordability of high-resolution satellite imageries had caused high reliability on the medium resolution satellite imageries (MRSI) in developing countries such as Nigeria. Also, the Normalized Difference Vegetation Index (NDVI) had been the most commonly used vegetation index for Vegetation Cover Mapping (VCM). It is pertinent to determine the most accurate vegetation index for VCM of a degraded forest environment in Nigeria despite the varied spatial and spectral resolutions of the MRSI. This study determined the appropriate vegetation indices from Landsat 8 and Sentinel 2A of degraded tropical forest in Ise Forest Reserve, Southwest Nigeria. Recent Landsat 8 and Sentinel 2A satellite imageries were acquired and pre-processed. The earlier was downscaled to ensure uniformity in spatial resolution with Sentinel 2A. Seven vegetation indices: NDVI, Enhanced Vegetation Index (EVI), Green Normalized Difference Vegetation Index (GNDVI), Pigment Specific Simple Ratio (PSSR), Soil Adjusted Vegetative Index (SAVI), Modified Soil Adjusted Vegetative Index (MSAVI) and Transformed Soil Adjusted Vegetative Index (TSAVI), were extracted from the datasets. Both Landsat 8 and Sentinel 2A have the same overall accuracy (98.00%) and kappa coefficients (0.96) in NDVI, SAVI and transformed SAVI. However, EVI (97.69% and 0.854), followed by GNDVI (91.50% and 0.802) extracted from Sentinel 2A outperformed NDVI (a common and widely used vegetation index) based on their overall accuracy and kappa coefficients respectively. The high performance of EVI (0.06 – 0.32) derived from Sentinel 2A despite the downscaling of Landsat 8 makes the consideration of spectral surface reflectance consequential. The enhanced capability and performance of Sentinel 2A in vegetation cover mapping should be more explored in developing economies with low affordability of commercial geospatial data.

Keywords: *Nigeria, Vegetation indices, Sentinel 2A, Landsat 8, Ise Forest Reserve*

Introduction

Over the years, the evolution of various vegetation indices had been instrumental in the quantification, prediction and reduction of environmental risks and ecological scarcities (Olmos-Trujillo *et al.*, 2020; Rokni and Gholizadeh, 2020; Zheng *et al.*, 2018). Ecological footprints are easier and better accounted for with the advancement and use of the vegetation index. The tropical forest area has been reduced drastically due to anthropogenic activities and nature over the past 10 years (Barlow *et al.*, 2016; Edwards *et al.*, 2019; Gizachew *et al.*, 2020). Biodiversity loss has attained significant intensity at various scales as a result of militating factors such as hunting, habitat destruction, overgrazing and indiscriminate bush burning [Nigeria Fifth National Biodiversity Report (NFNBR), 2015]. Based on these threats in sub-Saharan Africa, the vegetation cover assessment is imperative to understand the spatial heterogeneity of the remaining natural resources (Rajah *et al.*, 2019; Witt *et al.*, 2018).

Vegetation cover all over the world has been effectively mapped using different vegetation indices (VI) without prejudice to other methods (Greenberg *et al.*, 2006; Kamagata *et al.*, 2006; Okeke *et al.*, 2007; Xie *et al.*, 2008; Zheng *et al.*, 2006). The indices are computed according to the spectral radiance of the infrared and visible bands of the electromagnetic spectrum (Lein, 2012). Furthermore, remotely sensed image data have been instrumental in the computation of these indices. They are widely applied in ecological modelling, vegetation cover mapping and monitoring, and environmental modelling and monitoring (Tso and Mather, 2007). These data are acquired and processed through satellite remote sensing and Geographical Information System technology.

The high cost and non-affordability of the efficient remotely sensed image data - high-resolution satellite imageries - has caused high reliability on the medium resolution satellite imageries such as Landsat and Sentinel data in developing countries such as Nigeria. Despite the free availability of these MRSI, their usage for vegetation cover mapping in Nigeria is comparatively low to developed countries (Ibrahim and Kuta, 2015; Labib and Harris, 2018). Over 40 years, Landsat (a medium spatial resolution satellite imagery) has been widely used in vegetation cover mapping (Cord *et al.*, 2013; Jordan *et al.*, 2014; Ma *et al.*, 2013). Also, Sentinel 2A was a recently launched satellite in 2015 that provides 10m resolution for visible and near-infrared (NIR) bands (Labib and Harris, 2018). In terms of spatial resolution, Sentinel 2A is better than Landsat 8 imagery with a 15m panchromatic band, 30m visible and NIR bands (Drusch *et al.*, 2012; Roy *et al.*, 2014). Though the two sensors have different spectral characteristics, they are medium spatial resolution dataset, providing near-daily time series science and applications with latent to support global coverage (Zhang *et al.*, 2018).

Over time, several vegetation indices such as NDVI (Rouse *et al.*, 1974), EVI (Liu and Huete, 1995), GNDVI (Gitelson *et al.*, 1996), PSSR (Blackburn, 1998), SAVI (Huete, 1988), MSAVI (Richardson and Wiegand, 1977), TSAVI (Baret *et al.*, 1989) had been extracted from the two MRSI. They are usually computed using the multi-band threshold/spectral-based methods to differentiate the vegetated and non-vegetated areas (Sobrino *et al.*, 2004; Sonnentag *et al.*, 2007). These methods are the most widely used to map vegetated areas among other categories of vegetation cover mapping methods such as supervised classification (Friedl *et al.*, 2002) and machine learning techniques (Higginbottom *et al.*, 2018). Amidst the vegetation indices, NDVI is a commonly used index in vegetation cover mapping (Bhandari and Kumar, 2012; Xu and Su, 2017). It is calculated as a ratio difference between measured surface reflectance in the red and

near-infrared bands (Nageswara *et al.*, 2005). NDVI products have been extracted from Landsat and Sentinel data (Barichivich *et al.*, 2013; Silva *et al.*, 2013).

All these vegetation indices have one or more limitations for accurate vegetation cover mapping. For instance, NDVI is highly sensitive to low vegetation cover area and best suited for vegetation cover mapping of larger areas, but influenced by cloud cover, soil brightness, background noise and leaf canopy shadow (Gamon *et al.*, 1995; Grace *et al.*, 2007; Xue and Su, 2017). Based on these limitations, SAVI, MSAVI and TSAVI were developed to reduce the influence of soil background on the vegetation information to be extracted, but they have varied extraction capability (Wenlong, 2009; Xue and Su, 2017). Also, EVI had been considered to have improved sensitivity to vegetation cover mapping through de-coupling of atmospheric effects and background noise signal in a degraded environment (Huete *et al.*, 1999).

However, Li *et al.* (2017) and Zhang *et al.* (2018) opined that the Sentinel 2A data could be re-sampled to Landsat 8 resolution or the Landsat 8 data could be downscaled to Sentinel 2 resolution. In downscaling operation, different pansharpener techniques - Brovey Transform (BT), Fast Intensity-Hue-Saturation (FIHS), Smoothing Filter-based Intensity Modulation (SFIM) Additive Wavelet Transform (AWT) - had been employed to improve the MRSI's resolution and extract vegetation indices. According to Johnson *et al.* (2014), the FIHS pansharpener technique best enhanced the spatial information of an MSRI with no distortion of spectral information required for vegetation indices extraction. Based on this premise, this study incorporated the FIHS pansharpener technique to the spatial information of Landsat 8 for VCM of a degraded forest environment - Ise Forest Reserve in Nigeria.

Ise Forest Reserve is one of the protected areas located in the tropical hemisphere. It remains one of the remaining forest fragments in southwest Nigeria, militated with intense human anthropogenic activities such as farming, logging and hunting (Greengrass, 2006; Ogunjemite *et al.*, 2006). It is one of the priority conservation areas for the endangered Nigeria-Cameroun Chimpanzees (*Pan troglodytes ellioti*) in Nigeria with a degrading forest environment. In light of the aforementioned, this study aimed to determine the most accurate vegetation index(es) and MSRI (Landsat 8 OLI/TIRS and Sentinel 2A MSI) with the best performance for the VCM of a degraded forest environment - Ise Forest Reserve in Nigeria of degraded tropical forest in Nigeria.

Materials and Methods

Study area

The study was carried out in a tropical forest ecosystem of Ise Forest Reserve, southwest Nigeria (Figure 1). It is geographically located within 5° 20.804'E to 5° 25.331'E longitude and 7° 21.069'N to 7° 25.579'N latitude. The protected area is about 9km to the southern part of the reserve along Akure-Benin expressway from Uso community in Ondo State (Olaniyi *et al.*, 2016). The annual temperature is between 25°C – 28°C while generally, the minimum temperature is 19°C and the maximum temperature is 33°C. The annual precipitation is between 1200mm. Specifically, Ise Forest Reserve receives 1380mm of rainfall annually (Ikemeh, 2013). The rainfall is steady and spread almost evenly throughout the wet season (April-October). The Ogbese River flows by the western borders of Ise Forest Reserve and a relatively smaller perennial river flows within the reserve close to Eastern edge (Ikemeh, 2013).

Ise Forest Reserve is blessed with diverse fauna and flora species (Greengrass, 2006; Ogunjemite, 2011). Some of the flora species include *Gmelina arborea*, *Mansonia altissima*, *Tectona grandis*, *Alstonia boonei*, *Ceiba pentandra*, *Entandrophragma cylindricum*, *Terminalia ivorensis*, *Khaya ivorensis* and *Milicia excelsa*. Some of the fauna species include: primates like Mona monkey (*Cercopithecus mona*), Nigerian white-throated guenon (*Cercopithecus erythogaster pococki*), the Nigerian putty-nosed monkey (*Cercopithecus nictitans nilotus*), Red-capped mangabey (*Cercocebus torquatus*), Olive baboons (*Papio anubis*) and Nigeria-Cameroon Chimpanzee (*Pan troglodytes ellioti*) (Ogunjemite, 2011). Mammals like African forest elephant (*Loxodonta Africana cyclotis*), Forest buffalo (*Synerus caffernanus*) and Red river hog (*Potamochoerus porcus*). Some bird species like yellow-casqued hornbill (*Cerato gymnaelata*),

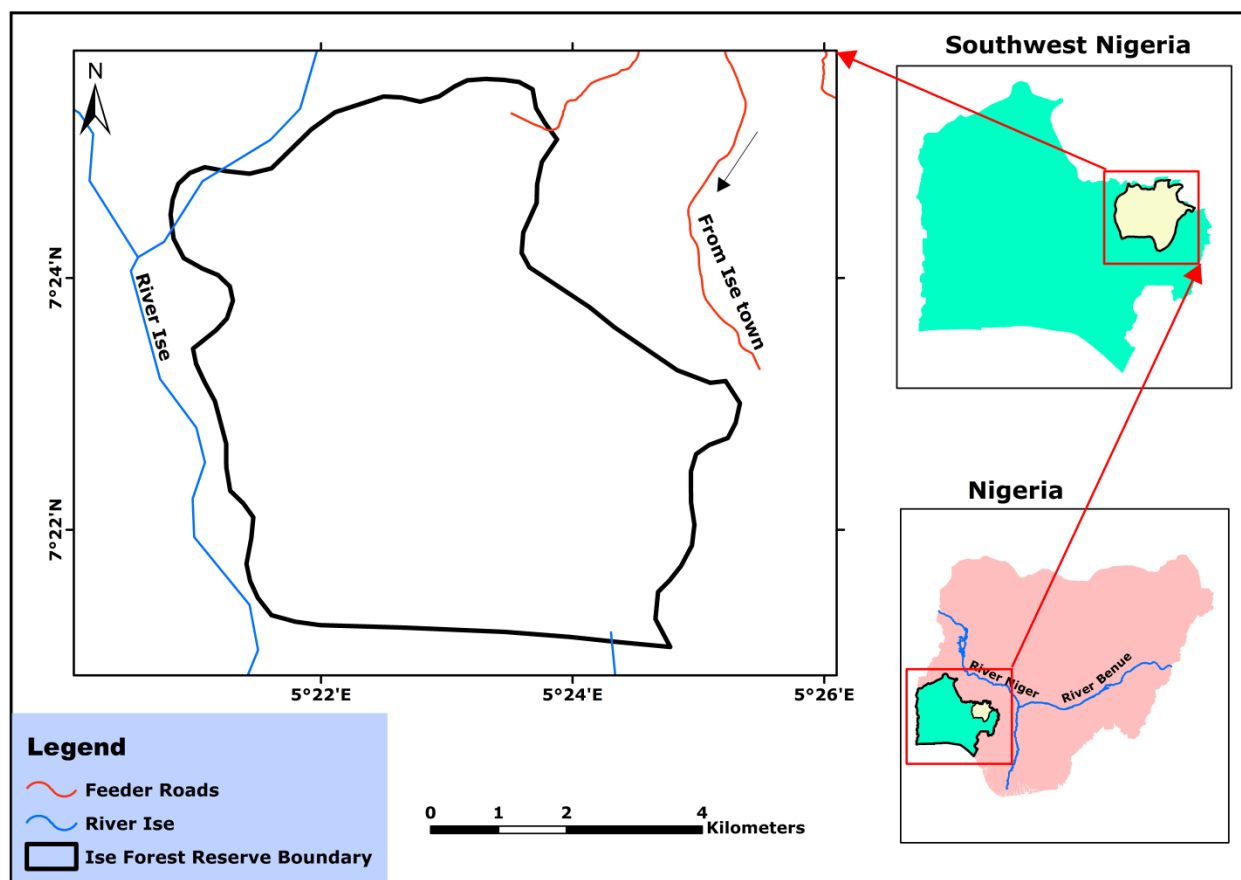


Figure 1: Ise Forest Reserve in Ekiti State, Southwest Nigeria

black casqued hornbills (*Cerato gymnaatrata*) and grey parrot (*Psittacus erythacus*) etc. (Ikemeh, 2013; Orimaye et al., 2016).

Image acquisition, pre-processing procedure and accuracy assessment

Landsat 8 OLI/TIRS Level-1 and Sentinel 2A satellite imageries were acquired from the United States Geological Service (USGS) archives with cloud cover less than 10% at 30 m and 10 m spatial resolutions respectively. These images were captured during the dry season (January 2018) in order to minimize the interference from cloud cover. The specifications of the satellite images acquired are presented in Table 1. The Sentinel 2A bands had already been atmospherically corrected with the bands in the dataset containing true top of Atmosphere

reflectance integer units. The raster was only converted to a floating-point according to European Space Agency (ESA) (2017) using the raster calculation tool of ArcGIS 10.4. According to Landsat 8 (L8) Data Users Handbook (2019), the Landsat 8 Level-1 digital numbers for each band were rescaled to top of atmosphere (TOA) reflectance (Equation 2) and true TOA reflectance (Equation 3)..

$$\text{Sentinel 2A}_{\text{Band}} = \frac{\text{Float}(\text{Band}_{\text{Integer}})}{10000} \quad (1)$$

Where,

$\text{Band}_{\text{Integer}}$ = Each Sentinel 2A band in integer

$$\text{TOA reflectance} = \text{RM}_s * \text{Float}(\text{DN band}) + \text{RA}_s \quad (2)$$

Where,

TOA = top of atmosphere

RM_s = Reflectance multiplicative scaling factor for the band (REFLECTANCEW_MULT_BAND_n from the metadata)

Table 1: Specifications of the satellite images acquired from United State Geological Survey in 2018.

Satellite properties	Landsat 8 Level 1T	Sentinel 2A Level 1C
Scene ID	LC81900552018023LGN00	S2A_MSIL1C_20180123T095311_N0206_R079_T31NGJ_20180123T134216.SAFE
Sensor ID	OLI/TIRS	MSI
Date acquired*	23rd January 2018	23rd January 2018
Sun elevation	51.0785212	-
Spatial resolution	30 x 30 m ²	10 x 10 m ²
Spectral bands	Blue, Green, Red, NIR, SWIR/Panchromatic	Blue, Green, Red, NIR/SWIR

*WRS Path: 190, WRS Row: 55 (Landsat 8); Tile ID: T31NGJ (Sentinel 2A)

OLI = Operational Land Imager; TIRS = Thermal Infrared Sensor; MSI = MultiSpectral Instrument, NIR = Near Infrared, SWIR = Short Wave Infrared

RA_s = Reflectance additive scaling factor for the band (REFLECTANCE_ADD_BAND_N from the metadata)

DN band = Level 1 pixel value in DN

$$\text{True TOA reflectance} = \frac{\text{TOA reflectance}}{\text{Sin}(\theta_{\text{SE}})} \quad (3)$$

Where,

TOA = top of atmosphere

θ_{SE} = Sun Elevation Angle (51.08°)

The processing was performed with the aid of the annotated supplementary information (radiometric and geometric calibration coefficients and georeferencing parameters) embedded in the dataset's support files. However, the pre-processing and enhancement (radiometric,

geometric and spectral corrections) of Landsat 8 and Sentinel 2A datasets (Kwang *et al.*, 2018) was performed using histogram equalization, haze and noise reduction functions in ERDAS Imaging 2014 software. The image enhancement is to improve its features' visual display without causing any spectral distortion (Olaniyi *et al.*, 2018). Additionally, the study area boundary and satellite datasets were subjected to change in spatial reference systems (coordinate transformation and datum projection). Specifically, they were transformed from the World Geodetic System 1984 (WGS84) to Minna Geographic Coordinate System and then projected from Minna Geographic Coordinate System to Minna Universal Transverse Mercator (UTM) 31N system.

Using the study area boundary, the images of the area were masked and obtained in the bands - blue, green, red, NIR, SWIR 1, SWIR 2 for Sentinel 2 and Landsat 8 data. The bands of Landsat were pansharpened and re-sampled to 10m using the image analysis and aggregate tools in ArcGIS 10.4. The pan-sharpening using the Fast Intensity-Hue-Saturation technique and re-sampling processes were implemented to ensure that the composite image of Landsat 8 has a spatial resolution of 10m with Sentinel 2 data which is 10m (Pushparaj and Hegde, 2017). Finally, the vegetation indices were extracted from the relevant bands of Sentinel 2 and Landsat 8 using the raster calculator tool in ArcGIS10.4 software. Hand-held GPS receiver was used to collect one hundred and fifty ground control points (GCPs) in January 2018 for accuracy assessment consisting of 100 GCPs and 50 GCPs for vegetated and non-vegetated areas respectively. Error matrices and kappa statistics were computed using the accuracy assessment tool in ERDAS Imagine 2014 software.

Computation of vegetation indices

Both satellite datasets (pan-sharpened/re-sampled Landsat 8 and Sentinel 2A) were subjected to spectral-based/multi-band threshold methods using the threshold value of 0.2 to differentiate the vegetated and non-vegetated areas

(Rouse *et al.*, 1973; Huete, 1988; Qi *et al.*, 1994; Gitelson and Merzlyak, 1998; Huete *et al.*, 2002; Sobrino *et al.*, 2004). The seven vegetation indices (Equations 4 - 10) were computed using the mathematical algorithms for various bands combinations as follows:

$$NDVI = \frac{NIR-R}{NIR+R} \quad (4)$$

Where R = Visible red reflectance

NIR = Near-infrared reflectance

$$GNDVI = \frac{NIR-G}{2NIR+G} \quad (5)$$

Where NIR = Near Infrared reflectance and

G = Green

$$PSSR = \frac{NIR}{R} \quad (6)$$

Where R = Visible red reflectance

NIR = Near-infrared reflectance.

$$SAVI = \frac{(1+L)*(NIR-R)}{(NIR+R+L)} \quad (7)$$

L = Canopy background adjustment factor (L = 0.5 - the most widely used value for intermediate vegetation cover)

$$MSAVI2 = \frac{(2*NIR+1-\sqrt{(2*NIR+1)^2-8*(NIR-R)})}{2} \quad (8)$$

Where R = Visible red reflectance

NIR = Near-infrared reflectance

$$TSAVI = \frac{a(NIR-aR-b)}{R+aNIR-ab} \quad (9)$$

Where R = Visible red reflectance

NIR = Near-infrared reflectance

a = Slope of soil line

b = Intercept of soil line

$$EVI = G * \frac{NIR-R}{NIR+C1*R-C2*BLUE+L} \quad (10)$$

G = Gain factor (2.5)

R = Visible red reflectance

NIR = Near-infrared reflectance

Blue = Visible blue reflectance

C1 and C2 = Coefficients of the aerosol resistance term

L = Canopy background adjustment factor

Results and Discussion

The comparison between the vegetative indices with their attributes of Landsat 8 and Sentinel 2A data for Ise Forest Reserve, Southwest Nigeria is presented in Table 2, Figures 2a and 2b. The results revealed that the PSSR and SAVI extracted from Landsat 8 recorded the highest vegetation (53.98 km², 95.09%) and non-vegetation (7.11 km², 12.52%) cover respectively and vice versa. For Sentinel 2A, the EVI (19.79 km², 34.86%) and modified SAVI (3.26 km², 5.74%) recorded the highest and least non-vegetation cover. Overall, the EVI extracted from Sentinel 2A recorded the highest vegetation (36.98 km², 65.14%) and non-vegetation (19.79 km², 34.86%) cover for both satellites.

The accuracy assessment of the vegetation indices extracted from Landsat 8 and Sentinel 2A of Ise Forest Reserve, Nigeria are presented in Table 3. NDVI extracted from Landsat 8 had the highest overall accuracy (67.14%) and kappa coefficient (0.587). Modified SAVI had the least overall accuracy (61.44%) and kappa coefficient (0.537). Also, EVI extracted from Sentinel 2A had the highest overall accuracy (97.69%) and kappa coefficient (0.854), followed by GNDVI with overall accuracy (91.50%) and kappa coefficient (0.802). But, modified SAVI had the least overall accuracy (70.88%) and kappa coefficient (0.620). Overall, EVI extracted from Sentinel 2A had the highest overall accuracy and kappa coefficient among the extracted vegetation indices from Landsat 8 and Sentinel 2A with range value (0.06 – 0.32).

The study revealed the capacity of the two medium resolution satellite imageries (Sentinel 2A and Landsat 8) to detect the vegetation cover of the forest ecosystem in southwestern Nigeria. The result showed a vast and varying vegetation cover during the dry season in Ise Forest Reserve for the year 2018. This is as a result of its location in the rainforest zone of southwestern Nigeria where many evergreens are supported. In reality, the heterogeneous vegetation or greenness is dominated by a vast area of cash crop plantations. According to Ogunjemite *et al.* (2006), logging, agricultural activities, flitching, hunting had posed serious ecological pressures (Greengrass, 2006). Even, scarcity of food resources and shrinkage of habitats had been substantiated to usually exist during the dry season (Olaniyi *et al.*, 2016). These challenges are anthropogenic and seasonal in nature. Notwithstanding, the protected area has great potential to sustain the propagation and conservation of its biodiversity.

It was observed that the vegetation indices extracted from Sentinel 2A revealed better output than Landsat based on the overall accuracy and kappa coefficient. The Enhanced vegetative index (EVI) extracted from Sentinel 2A is the best vegetation index for determining vegetation cover in Ise Forest Reserve. In addition, GNDVI extracted from Sentinel 2A presented a better accuracy and option for vegetation cover determination. In this case, the reason might not be the spatial resolution which does influence the classification algorithm processes (Benz *et al.*, 2004; Blaschke, 2010), but the spectral surface reflectance of the dataset. Zhang *et al.* (2018) opined that the Multispectral Instrument (MSI) surface reflectance of Sentinel 2A is usually greater than the OLI surface reflectance of Landsat 8 for all the bands except the green, red, and NIR bands.

However, the mathematical algorithm of EVI consisted of the blue band. Thus, the surface reflectance of the blue band in the computation of EVI could have been responsible for its higher performance in the vegetation cover mapping of the degraded tropical forest. Moreover, the Enhanced vegetation index (EVI) is an optimized vegetation index designed to enhance the vegetation signal with improved sensitivity in high biomass regions. Also, EVI improved vegetation monitoring through the decoupling of the canopy background signal and a reduction in atmosphere influences (Huete and Justice, 1999). Huete *et al.* (2006) reported one of the most successful applications of EVI in a monotonous growing season of the Amazon forest where vegetation growth has no particular pattern. They revealed contrary to popular notion using MODIS EVI that the Amazon forest does exhibit distinct growth during the dry season.

Although the chlorophyll sensitive NDVI had been the widely used vegetation index, EVI is more responsive to canopy structural variations and more applicable to the heterogeneous vegetation of Ise Forest Reserve with predominantly plantations. In the study, the overall accuracy and kappa coefficient of NVDI extracted from Sentinel 2A was greater than Landsat 8. This could be due to the assertion of Zhang *et al.* (2018) that the MSI surface NDVI from Sentinel 2A was greater than the OLI surface NDVI from Landsat 8. Moreover, NDVI had a closer accuracy with EVI, PSSR, SAVI and transformed SAVI extracted from Landsat 8. It implied that EVI, PSSR, SAVI and transformed SAVI extracted from Landsat 8 can also be used instead of the commonly used NDVI in the vegetation cover mapping of degraded tropical forest. This opinion supported the view of Ali *et al.* (2018) that SAVI had a stronger correlation with NDVI, and it is the best vegetation index suited for the estimation and monitoring of vegetation cover in the Jeffara Plain, Libya.

On the other hand, the form of radiometric and spatial pre-processing operations on satellite dataset with different spatial resolution could not enhance the accuracy of the extracted vegetation indices. Despite the downscaling operation on the Landsat 8, the extracted vegetation indices had a lesser overall accuracy and kappa coefficient to those of Sentinel 2A. This could be due to the information enhancing capability of Sentinel 2A in vegetation cover assessment as reported by Addabbo *et al.* (2016). They observed that vegetation indices extracted from Sentinel 2 indices provided the highest values due to its ability to discriminate the different optical/multispectral sensors. Also, Watanabe *et al.*, (2017) submitted that the band ratios in NIR-red algorithms in Sentinel 2A imagery performed best in the estimation of chlorophyll-a than Landsat 8 in Barra Bonita reservoir, Brazil.

Table 2: Comparative vegetation indices' attributes of Ise Forest Reserve, Southwest Nigeria in 2018.

Vegetation indices/Attributes	Landsat 8		Sentinel 2A	
	Area cover (Km²)	Proportion (%)	Area cover (Km²)	Proportion (%)
NDVI				
Non-vegetated area	3.47	6.12	3.53	6.22
Vegetated area	53.30	93.88	53.24	93.78
EVI				
Non-vegetated area	5.63	9.91	19.79	34.86
Vegetated area	51.14	90.09	36.98	65.14
GNDVI				
Non-vegetated area	6.56	11.56	15.00	26.43
Vegetated area	50.21	88.44	41.77	73.57
PSSR				
Non-vegetated area	2.79	4.91	7.32	12.89
Vegetated area	53.98	95.09	49.45	87.11
SAVI				
Non-vegetated area	7.11	12.52	7.37	12.99
Vegetated area	49.66	87.48	49.40	87.01
TRANSFORMED SAVI				
Non-vegetated area	8.57	15.09	8.64	15.22
Vegetated area	48.20	84.91	48.13	84.78
MODIFIED SAVI				
Non-vegetated area	3.81	6.72	3.26	5.74
Vegetated area	52.96	93.28	53.51	94.26

Table 3: Accuracy assessment of the vegetation indices extracted from Landsat 8 and Sentinel 2A of Ise Forest Reserve, Nigeria in 2018.

Vegetation indices (VI)	VI range values	Landsat 8		Sentinel 2A		
		Overall accuracy	Kappa coefficient	VI range values	Overall accuracy	Kappa coefficient
NDVI	0.10 – 0.22	67.14	0.587	0.15 – 0.51	71.36	0.623
EVI	0.16 – 0.37	67.02	0.586	0.06 – 0.32	97.69	0.854
GNDVI	0.10 – 0.17	63.28	0.553	0.07 – 0.25	91.50	0.802
PSSR	0.13 – 0.38	67.04	0.586	0.12 – 0.31	78.03	0.682
SAVI	0.14 – 0.30	66.81	0.584	0.08 – 0.36	78.13	0.683
TRANSFORMED SAVI	0.15 – 0.24	66.45	0.581	0.14 – 0.36	80.36	0.703
MODIFIED SAVI	0.16 – 0.28	61.44	0.537	0.13 – 0.38	70.88	0.620

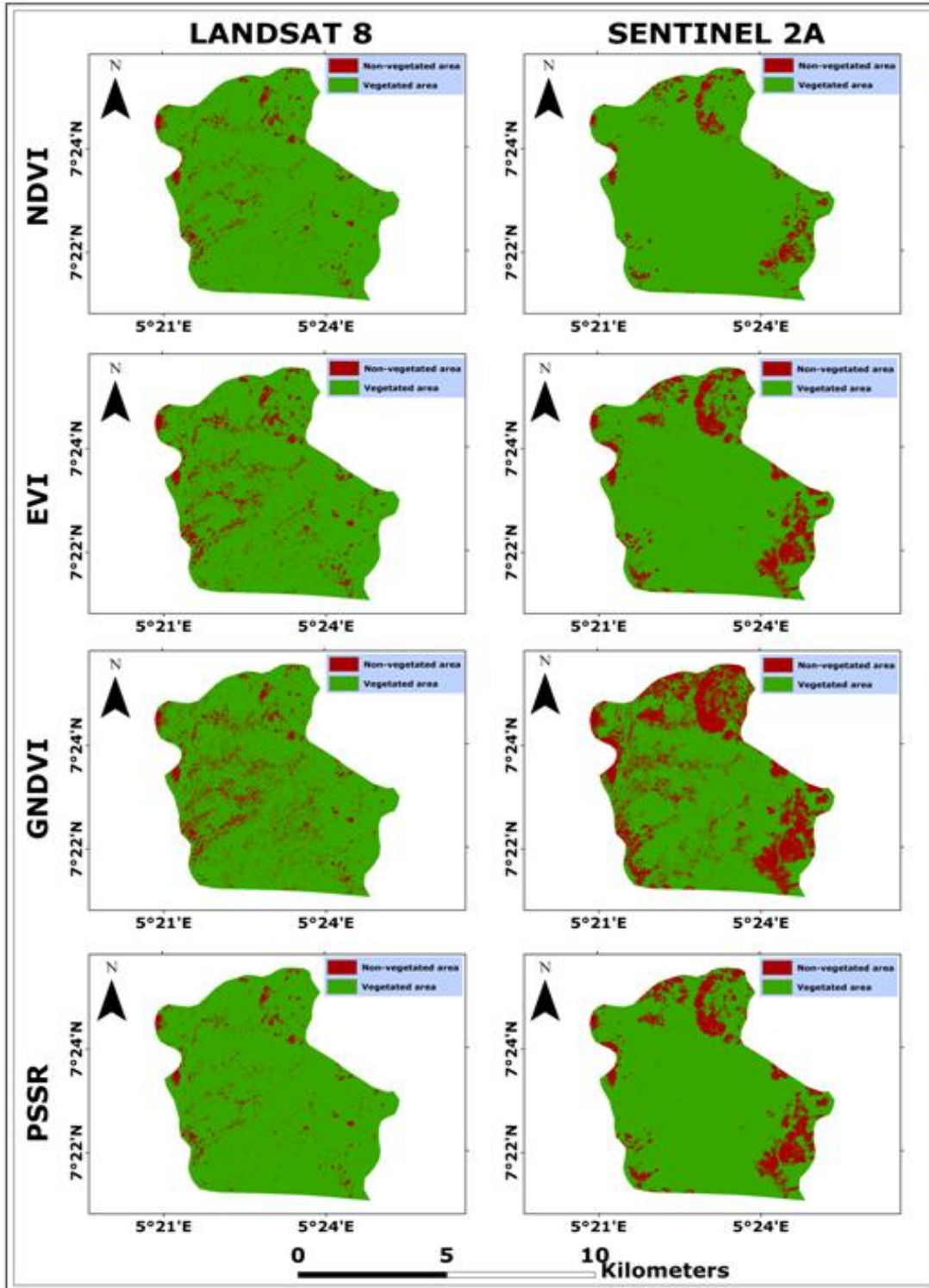


Figure 2a: Comparison between the vegetation indices of Landsat 8 and Sentinel 2A data for Ise Forest Reserve, Southwest Nigeria.

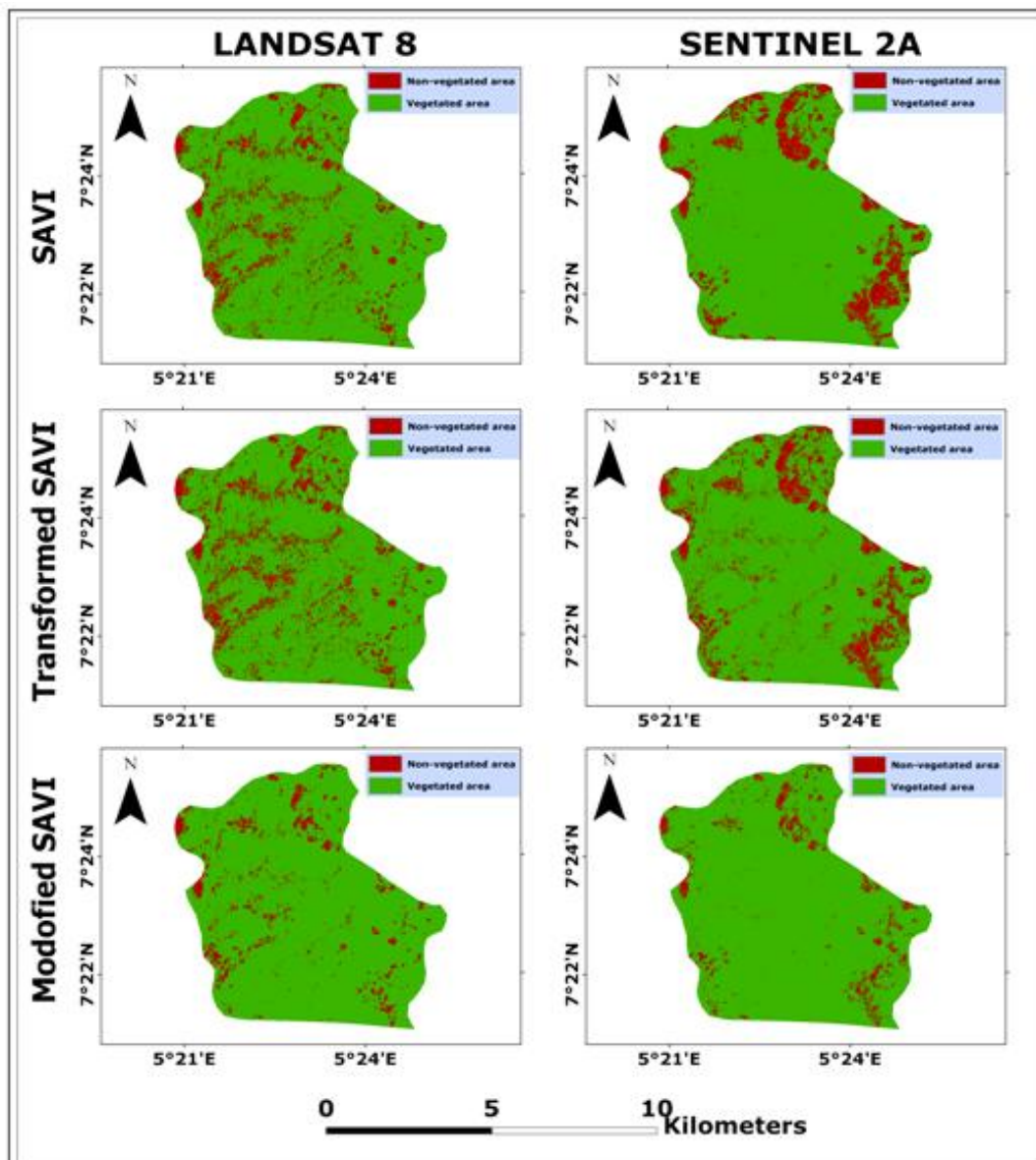


Figure 2b: Comparison between the vegetative indices of Landsat 8 and Sentinel 2A data for Ise Forest Reserve, Southwest Nigeria.

Conclusion

The study has demonstrated that Sentinel 2A satellite imagery performs better than Landsat 8 satellite imagery despite the uniformity in their spatial resolution. Basically, Sentinel 2A had a higher performance (EVI and GNDVI) in the vegetation cover mapping of Ise Forest Reserve. The high performance of EVI derived from Sentinel 2A despite the downscaling of Landsat 8 makes the consideration of spectral surface reflectance consequential. Therefore, the findings had demonstrated the potential of EVI and GNDVI extracted from Sentinel 2A above the commonly used NDVI. The EVI, PSSR, SAVI and transformed SAVI extracted from either Landsat 8 can also be used instead of the commonly used NDVI in the vegetation cover mapping operations. Muchmore, the inaccessibility to very high and high-resolution satellite datasets due

to its high cost could pose no limitations to vegetation health assessment research. Therefore, it is recommended that the enhanced capability and performance of Sentinel 2 in vegetation cover mapping should be more explored in developing economies with low affordability of commercial geospatial data.

Acknowledgements

Our profound gratitude goes to the Department of Forestry in the Ministry of Environment, Ekiti State for granting access to the study area. The comments and suggestions of the reviewers and the editorial team are highly appreciated.

References

- Addabbo, P., Focareta, M., Marcuccio, S., Votto, C., and Ullo, S.L. (2016). Contribution of Sentinel 2 data for applications in vegetation monitoring. *Acta Imeko* 5 (2), 44-54.
- Ali, A., Hallett, S and Brewer, T. (2018). Using vegetation indices for the estimation and production of vegetation cover maps in the Jeffara Plain, Libya. *IOSR Journal of Environmental Science, Toxicology and Food Tech* 12 (2), 23-28.
- Baret, F., Guyot, G. and Major, D.J. (1989). TSAVI: A vegetation index which minimizes soil brightness effects on LAI and APAR estimation,” in *Proceedings of the 12th Canadian Symposium on Remote Sensing Geoscience and Remote Sensing Symposium* 1355–1358.
- Barichivich, J. (2013). Large scale variations in the vegetation growing season and annual cycle of atmospheric CO₂ at high northern latitudes from 1950 to 2011. *Global change biology*.
- Barlow, J., Lennox, G. D., Ferreira, J., Berenguer, E, Lees, A. C., Nally, R. M., Thomson, J. R., Ferraz, S. B. and Louzada, J. (2016). Anthropogenic disturbance in tropical forests can double biodiversity loss from deforestation. *Nature*. <https://doi.org/10.1038/nature18326>
- Benz, U.C., Hofmann, P., Willhauck, G., Lingenfelder, I, and Heynen, M. (2004). Multi-resolution, object-oriented fuzzy analysis of remote sensing data for GIS-ready information. *ISPRS Journal of Photogrammetry and Remote Sensing* 58 (3), 239–258.
- Bhandari, A.K. and Kumar, A. (2012). Feature Extraction using Normalized Difference Vegetation Index (NDVI): A Case Study of Jabalpur City. *Proceedings of Communication, Computing & Security. Procedia Technology* 6, 612– 621,
- Blackburn, G.A. (1998). Quantifying chlorophylls and carotenoids at leaf and canopy scales: an evaluation of some hyperspectral approaches. *Remote Sensing of Environment* 66(3), 273–285
- Blaschke, T. (2010). Object based image analysis for remote sensing. *ISPRS Journal of Photogrammetry and Remote Sensing* 65 (1), 2–16.
- Cord, A.F., Meentemeyer, R.K., Leitao, P.J., Vaclavik, T. Whittaker, R. (2013). Modelling species distributions with remote sensing data: bridging disciplinary perspectives. *Journal of Biogeography* 40 (12), 2226-2227.
- David P. E., Jacob B. S., Simon C. M., Zuzana B., Lian P.K., and David S. W. (2019). Conservation of Tropical Forests in the Anthropocene. *Current Biology Review* 29, 1008–1020.

- Drusch, M., Del Bello, U., Carlier, S., Colin, O., Fernandez, V., Gascon, F. and Meygret, A. (2012). Sentinel-2: ESA's European Journal of Remote Sensing 239 optical high-resolution mission for GMES operational services. *Remote Sensing of Environment* 120, 25–36.
- European Space Agency (ESA), (2017).; Sentinel-2 Spatial Resolution. Cited at: https://earth.esa.int/web/European_Space_Agency_sentinel/user-guides/sentinel-2-msi/resolutions/spatial.
- Edwards, D.P., Socolar, J.B., Mills, S.C., Burivalova, Z., Koh, L.P., Wilcove, D.S. (2019). Conservation of Tropical Forests in the Anthropocene. *Current Biology Review* 29, 1008–1020.
- Friedl, M.A., McIver, D.K., Hodges, J.C.F., Zhang, X.Y., Muchoney, D., Strahler, A.H., Woodcock, C.E., Gopal, S., Schneider, A., Cooper, A., et al. (2002). Global land cover mapping from MODIS: Algorithms and early results. *Remote Sens. Environ* 83, 287–302..
- Gamon, J.A., Field, C.B., Goulden, M.L., Griffin, K.L., Hartley, A.E., Joel, G., Penuelas, J., Valentini, R. (1995). Relationships between NDVI, canopy structure, and photosynthesis in three Californian vegetation types. *Ecological Applications* 5(1), 28–41. <https://doi.org/10.2307/1942049>.
- Gitelson, A. and Merzlyak, M. (1998). Remote Sensing of Chlorophyll Concentration in Higher Plant Leaves." *Advances in Space Research* 22, 689-692.
- Gitelson, A.A., Kaufman, Y. and Merzlyak, M.N. (1996). Use of a green channel in remote sensing of global vegetation from EOS-MODIS. *Remote Sensing Environment* 58, 289-298.
- Gizachew, B., Rizzi, J., Shirima, D.D., and Zahabu, E. (2020). Deforestation and Connectivity among Protected Areas of Tanzania. *Forests* 11 (2), 170; <https://doi.org/10.3390/f11020170>
- Grace, J., Nichol, C., Disney, M., Lewis, P., Quaife, T. and Bowyer, P. (2007). Can we measure terrestrial photosynthesis from space directly, using spectral reflectance and fluorescence?" *Global Change Biology* 13(7), 1484–1497.
- Greenberg J. A., Dobrowski S. Z., Ramirez C. M., Tuil J. L., and Ustin S. L. (2006). A Bottom-up Approach to Vegetation Mapping of the Lake Tahoe Basin Using Hyperspatial Image Analysis, *Photogrammetric Engineering & Remote Sensing* 72 (5), 581-589.
- Greengrass, E.J. (2006). *A survey of Chimpanzee in South-West Nigeria*. NCF-WCS Biodiversity Research Programme. Calabar, Nigeria. 51pp.
- Higginbottom, T.P., Symeonakis, E., Meyer, H. and Van Der Linden, S. (2018). Mapping fractional woody cover in semi-arid savannahs using multi-seasonal composites from Landsat data. *ISPRS J. Photogramm. Remote Sens.* 139, 88–102.
- Huete, A.R. (1988). A Soil-Adjusted Vegetation Index (SAVI). *Remote Sensing of Environment* 25, 295-309.
- Huete, A.R., Justice C. and Leeuwen, W.V. (1999). MODIS vegetation index (MOD13) algorithm theoretical basis document. Ver. 3. University of Arizona, Tuscon, USA, 120pp.
- Huete, A.R., Didan, K., Shimabukuro, Y.E., Ratana, P., Saleska, S.R., Hutyrá, L.R., Yang, W., Nemani, R.R., and Myneni, R. (2006). Amazon rainforests green-up with sunlight in dry season. *Geophys. Res. Lett.* 33, L06405

- Huete, A.R., Didan, K., Miura, T., Rodriguez, E.P., Gao, X., Ferreira, L.G. (2002). Overview of the Radiometric and Biophysical Performance of the MODIS Vegetation Indices. *Remote Sensing of Environment* 83 (1-2), 195–213. [https://doi.org/10.1016/s0034-4257\(02\)00096-2](https://doi.org/10.1016/s0034-4257(02)00096-2).
- Ibrahim, S. and Kuta, A.A. (2015). Challenges in using Geographic Information Systems (GIS) to Understand and Control Crime in Nigeria. *IOSR Journal of Humanities and Social Science* 20 (3), 43-48.
- Ikemeh, R.A. (2013). Status Survey to determine the Population Viability of the Nigerian Cameroon Chimpanzees in Nigerian Lowland Rainforests of Southern Western Nigeria: Ise forest reserve and the Idanre forest cluster. A report to the Ondo and Ekiti State Governments, SW/ Niger Delta Forest Project, Nigeria. pp60.
- Johnson, B.A., Scheyvens, H., Shivakoti, B.R. (2014). An ensemble pansharpener approach for finer-scale mapping of sugarcane with Landsat 8 imagery. *Int. J. Appl. Earth Obs. Geoinf.* 33, 218–225. <http://dx.doi.org/10.1016/j.jag.2014.06.003>.
- Jordan, Y.C. (2014). Traits of surface water pollution under climate and land use changes: A remote sensing and hydrological modeling approach. *Earth-Science Reviews* 128, 181-195.
- Kamagata N., Hara K., Mori M., Akamatsu Y., Li Y., Hoshino Y. (2006). A New Method of Vegetation Mapping by Object-Based Classification Using High Resolution Satellite Data. *Journal of the Japan society of photogrammetry and remote sensing* 45 (1), 43 – 49.
- Kwang, C., Osei, E.M., and Amoah, A.S., 2018. Comparing of Landsat 8 and Sentinel 2A using Water Extraction Indexes over Volta River. *Journal of Geography and Geology* 10 (1), 1-7
- Labib, S.M., and Harris, A. (2018). The potentials of Sentinel-2 and LandSat-8 data in green infrastructure extraction, using object-based image analysis (OBIA) method, *European Journal of Remote Sensing* 51 (1), 231-240.
- Landsat 8 (L8) Data Users Handbook, (2019). Department of the Interior U.S. Geological Survey. https://prd-wret.s3.us-west2.amazonaws.com/assets/palladium/production/atoms/files/LSDS-574_L8_Data_Users_Handbook-v5.0.pdf
- Lein, J.K. (2012). Environmental Sensing Analytical Techniques for Earth Observation. Springer Nature America, Inc.
- Li, Z., Zhang, H.K., Roy, D.P., Yan, L., Huang, H., Li, J. (2017). Landsat 15-m panchromatic-assisted downscaling (LPAD) of the 30-m reflective wavelength bands to Sentinel-2 20-m resolution. *Remote Sensing* 9 (7), 755.
- Liu, H.Q. and Huete, A.R. (1995). A feedback based modification of the NDV I to minimize canopy background and atmospheric noise. *IEEE Transactions on Geoscience and Remote Sensing* 33, 457-465.
- Ma, X., Huete, A., Yu, Q., Coupe, N.R., Davies, K., Broich, M., Ratana, P., Beringer, J., Hutley, L.B., Cleverly, J., Boulain, N., Eamus, D. (2013). Spatial patterns and temporal dynamics in savanna vegetation phenology across the North Australian Tropical Transect. *Remote sensing of Environment* 139, 97-115.
- Nageswara, P.P.R., Shobha, S.V., Ramesh, K.S. and Somashekhar, R.K. (2005). Satellite-based assessment of Agricultural drought in Karnataka State. *Journal of the Indian society of remote sensing* 33 (3), 429-434.

- Nigeria Fifth National Biodiversity Report (NFNBR), (2015). Retrieved May 8, 2020 from <https://www.cbd.int/doc/world/ng/ng-nr-05-en.pdf/>
- Ogunjemite, B.G. (2011). Chimpanzees (*Pan troglodytes*) populations in southwestern Nigeria. *Journal of Sustainable Development in Africa* 13 (2), 60-73.
- Ogunjemite, B.G., Afolayan, T.A., Agbelusi, E.A. and Onadeko, S.A. (2006). Status survey of chimpanzees in the forest zone of southwestern Nigeria. *Acta Zoologica Sinica* 52 (6), 1009-1014.
- Okeke, F.I., Nwosu, K.I., and Mohammed, S.O. (2007). A GIS Enhanced AgroEcological Zoning for Nigeria using Satellite Imageries: Prospects and Possibilities. *Nigerian Journal of Space Research* 4, 149-164.
- Olaniyi, O.E., Kekere, T.C., and Ogunjemite, B.G. (2016). Quantifying the host communities' dependence on Chimpanzees' habitat of Ise Forest Reserve, Southwest Nigeria. *Proceedings of Forest and Forest products Society* 5, 305-311.
- Olaniyi, O.E., Ogunjemite, B.G., Akindele, S.O., and Sogbohossou, E.A. (2018). Temporal and distance decay analysis of land use/land cover around ecotourism hotspots: Evidence from Pendjari National Park, Benin. *GeoJournal*. 85(1): 53-66.
<https://doi.org/10.1007/s10708-018-9948-2>
- Olmos-Trujillo, E., González-Trinidad, J., Júnez-Ferreira, H., Pacheco-Guerrero, A., Bautista-Capetillo, C., Avila-Sandoval, C. and Galvan-Tejada, E. (2020). Spatio-Temporal Response of Vegetation Indices to Rainfall and Temperature in a Semiarid Region. *Sustainability* 12 (5), 1939. <https://doi.org/10.3390/su12051939>.
- Orimaye J.O., Olumide O.O., Okosodo, E.F., Victor A.O., and Agbelusi T.O. (2016). Butterfly Species Diversity in Protected and Unprotected Habitat of Ise Forest Reserve, Ise Ekiti, Ekiti State. *Advances of Ecology* 1-5. <http://dx.doi.org/10.1155/2016/7801930>
- Pushparaj, J., and Hegde, A.V. (2017). Comparison of various pan-sharpening methods using Quickbird-2 and LandSat-8 imagery. *Arabian Journal of Geosciences* 10 (5), 119.
<https://doi.org/10.1007/s12517-017-2878-3>
- Qi, J., Chehbouni, A., Huete, A., Kerr, Y. and Sorooshian, S. (1994). A Modified Soil Adjusted Vegetation Index. *Remote Sensing of Environment* 48, 119-126.
- Rajah, P., Odindi, J., Mutanga, O. and Kiala, Z. (2019). The utility of Sentinel-2 Vegetation Indices (VIs) and Sentinel-1 Synthetic Aperture Radar (SAR) for invasive alien species detection and mapping. *Nature Conservation* 35, 41–61.
<https://doi.org/10.3897/natureconservation.35.29588>
- Richardson, A.J., and Wiegand, C. (1977). Distinguishing vegetation from soil background information. *Photogrammetric Engineering & Remote Sensing* 43 (12), 1541–1552.
- Rokni, K. and Gholizadeh, M. (2020). Investigating the applicability of conventional vegetation indices for vegetation change detection in different environmental conditions. *Journal of Plant Ecosystem Conservation* 7(15), 125-140
- Rouse Jr., J.W., Haas, R., Schell, J. and Deering, D. (1974). Monitoring vegetation systems in the great plains with erts. NASA Special Publication 351, 309.
- Rouse, J., Haas, R., Schell, J. and Deering, D. (1973). *Monitoring Vegetation Systems in the Great Plains with ERTS*. Third ERTS Symposium, NASA, 309-317.
- Roy, D.P., Wulder, M.A., Loveland, T.R., Woodcock, C.E., Allen, R.G., Anderson, M.C., and Scambos, T.A. (2014). Landsat-8: Science and product vision for terrestrial global change research. *Remote Sensing of Environment* 145, 154–172.

- Silva, F.B., Shimabukuro, Y.E., Aragao, Luiz E.O.C., Anderson, L.O., Pereira, G., Cardozo, F., Arai, E. (2013). Large-scale heterogeneity of Amazonian phenology revealed from 26-year long AVHRR/NDVI time series. *Environmental Research Letters* 8 (2), 024011.
- Sobrino, J.A., Jiménez-Muñoz, J.C. and Paolini, L. (2004). Land surface temperature retrieval from LANDSAT TM 5. *Remote Sens. Environ.* 90, 434–440
- Sonnentag, O., Chen, J.M., Roberts, D.A., Talbot, J., Halligan, K.Q. and Govind, A. (2007). Mapping tree and shrub leaf area indices in an ombrotrophic peatland through multiple endmember spectral unmixing. *Remote Sens. Environ* 109, 342–360.
- Tso, B., and Mather, P. (2007). Classification methods for remotely sensed data. 1st ed. Boca Raton, Fla.: CRC/Taylor & Francis.
- Watanabe, F., Alcântara, E., Rodrigues, T., Rotta, L., Bernardo, N., and Imai, N. (2017). Remote sensing of the chlorophyll-a based on OLI/Landsat-8 and MSI/Sentinel-2A (Barra Bonita reservoir, Brazil).
- Wenlong, D.L. (2009). Vegetation index controlling the influence of soil reflection. <http://www.paper.edu.cn/releasepaper/content/200906-376>.
- Witt, A., Beale, T., Wilgen, V. and Brian, W. (2018). An assessment of the distribution and potential ecological impacts of invasive alien plant species in eastern Africa. *Transactions of the Royal Society of South Africa*.
- Xie, Y., Sha, Z., Yu, M. (2008). Remote sensing imagery in vegetation mapping: a review. *J. Plant Ecol.* 1, 9–23. <http://dx.doi.org/10.1093/jpe/rtn005>
- Xue, R and Su, B. (2017). Significant Remote Sensing Vegetation Indices: A Review of Developments and Applications. *Journal of Sensors* 2017, 1–17. <https://doi.org/10.1155/2017/1353691>.
- Zhang, H.K., Roy, D.P., Yan, L., Li, Z., Huang, H., Vermote, Skakun, S., and Roger, J. (2018). Characterization of Sentinel-2A and Landsat-8 top of atmosphere, surface, and nadir BRDF adjusted reflectance and NDVI differences. *Remote Sensing of Environment* 215, 482–494.
- Zheng, C.H., Zeng, C.S., and Chen, Z.Q. (2006). A study on the changes of landscape pattern of estuary wetlands of the Minjiang river. *Wetland Science* 4, 29 -35.
- Zheng, Y., Han, J., Huang, Y., Fassnacht, S.R., Xie, S., Lv, E., and Chen, M. (2018). Vegetation response to climate conditions based on NDVI simulations using stepwise cluster analysis for the Three-River Headwaters region of China. *Ecol. Indic.* 92, 18–29.